



This is a repository copy of *Implications of model uncertainty for investment decisions to manage intermittent sewer overflows*.

White Rose Research Online URL for this paper:
<https://eprints.whiterose.ac.uk/171313/>

Version: Accepted Version

Article:

Sriwastava, A.K., Torres-Matallana, J.A., Schellart, A. et al. (2 more authors) (2021) Implications of model uncertainty for investment decisions to manage intermittent sewer overflows. *Water Research*, 194. 116885. ISSN 0043-1354

<https://doi.org/10.1016/j.watres.2021.116885>

Article available under the terms of the CC-BY-NC-ND licence
(<https://creativecommons.org/licenses/by-nc-nd/4.0/>).

Reuse

This article is distributed under the terms of the Creative Commons Attribution-NonCommercial-NoDerivs (CC BY-NC-ND) licence. This licence only allows you to download this work and share it with others as long as you credit the authors, but you can't change the article in any way or use it commercially. More information and the full terms of the licence here: <https://creativecommons.org/licenses/>

Takedown

If you consider content in White Rose Research Online to be in breach of UK law, please notify us by emailing eprints@whiterose.ac.uk including the URL of the record and the reason for the withdrawal request.



eprints@whiterose.ac.uk
<https://eprints.whiterose.ac.uk/>

1 **Implications of model uncertainty for investment decisions** 2 **to manage intermittent sewer overflows**

3
4 Ambuj Kumar Sriwastava¹, J. A. Torres-Matallana², Alma Schellart³, Ulrich Leopold², Simon Tait³

5
6
7 ¹Department of Automatic Control and Systems Engineering, University of Sheffield, Portobello Street,
8 S1 3JD Sheffield, United Kingdom (Email: a.k.sriwastava@sheffield.ac.uk)

9 ²Department for Environmental Research and Innovation, Luxembourg Institute of Science and
10 Technology, 5, avenue des Hauts-Fourneaux, L-4362, Esch-sur-Alzette, Luxembourg

11 ³Department of Civil and Structural Engineering, University of Sheffield, Mappin Street, S1 3JD Sheffield,
12 United Kingdom

13 14 15 **Abstract**

16 Uncertainty in urban drainage modelling studies presents challenges to decision makers with
17 limited investment resources attempting to achieve regulatory compliance for intermittent
18 discharges from Combined Sewer Overflows. This paper presents the development of a new
19 decision-making approach to address two key challenges encountered when attempting to
20 manage sewer overflows, these are (i) the implications of different risk preferences of
21 individuals for investment decisions; and (ii) how to utilize information on uncertainties in
22 system performance predictions due to input or parameter uncertainty while comparing
23 decision alternatives. The developed decision-making approach uses a multi-objective
24 decision formulation to analyse the trade-off between investment and predicted system
25 performance under uncertainty while accounting for risk preferences of the individual
26 decision maker. The proposed uncertainty based decision-making approach is able to
27 incorporate any threshold-based regulatory criteria for intermittent sewer overflows and is
28 illustrated using a case study catchment in Luxembourg. The results from this case study
29 highlight the significant impact of individuals' risk preferences on the level of investment
30

31 recommended to comply with threshold-based regulatory criteria. It was demonstrated that
32 differing levels of risk-averseness can result in a substantial increase in investment cost for
33 solutions that are regulatory compliant. This paper demonstrates the need for water
34 companies to rigorously define a corporate risk preference strategy to ensure consistent
35 investment decisions across their operations; otherwise, individual preferences may cause
36 significant over-investment to meet the same regulatory goals.

37

38

39 **Keywords**

40 Buffered probability of exceedance; Decision making under modelling uncertainty;

41 Intermittent sewer overflows; Investment cost; Risk preference.

42

43 **1. Introduction**

44 Environmental regulators may impose performance standards for the operation of overflow
45 structures in combined sewer systems, which release excess wastewater to receiving water
46 bodies when the flow capacity of the urban drainage system is exceeded. For example, the
47 Urban Pollution Management Manual in the United Kingdom specifies concentration-duration-
48 frequency based criteria for ammonia concentrations and dissolved oxygen (DO) levels to
49 mitigate ecological impacts caused by combined sewer overflow (CSO) spills (Foundation for
50 Water Research, 2012). However, the criterion to evaluate the performance of CSOs is not
51 uniform across EU countries (De Toffol, 2006; Dirckx et al., 2011; Milieu, 2016). For example,
52 in Belgium, Denmark and Netherlands, regulations based on annual overflow frequency are
53 enforced while in Germany the criterion for CSO spills considers the overflow volume (Dirckx
54 et al., 2011). Water utilities are required to comply with the regulations applicable to their
55 country, and failing to do so can result in financial penalties and reputational damage, e.g. the
56 UK water utility Thames Water was recently fined 20 million pounds for releasing untreated
57 sewage via overflows in contravention of its discharge consents (Environment Agency, 2017).

58 Therefore, the successful management of sewer systems involves investment and operational
59 decisions which are often risk-averse in character because they aim to “eliminate” the risk of
60 non-compliance. More specifically, such decision-making aims to identify, test and implement
61 solutions or strategies which minimize the risk of non-compliance, while satisfying constraints
62 such as available budgets, land use and other planning or technical system constraints.
63 Hydrodynamic network models are often used to assess the performance of the proposed
64 solutions and strategies (Delelegn et al., 2011). However, it has been established that there is
65 significant predictive uncertainty when using such hydrodynamic models (e.g. Deletic et al.,
66 2012; Schellart et al., 2010; Thorndahl and Willems, 2008). Yu et al. (2017) mentioned that in
67 addition to the system performance modelling uncertainty, uncertainty in cost estimation also
68 poses challenges in finding optimal solutions that satisfy the objectives and constraints set by
69 the decision maker. Several studies which explicitly account for modelling uncertainty when
70 making decisions to mitigate the negative impact of CSO spills have been reported (e.g. Reda
71 and Beck (1997), Portielje et al. (2000), Korving et al. (2009), Meng et al. (2016)). Lin et al.
72 (2020), Mohammadiun et al. (2018), Yu et al. (2017), and Zhang et al. (2019) are recent studies
73 which applied uncertainty based evaluation of decision alternatives for the mitigation of flood
74 risk from urban sewer systems.

75 Although the aforementioned studies have incorporated uncertainty in the prediction of urban
76 drainage processes in some form, they have not fully captured the uncertainty in the system
77 performance. For example, Reda and Beck (1997) only considered extreme values and Korving
78 et al. (2009) used the probability of exceeding a threshold. Meng et al. (2016) did consider the
79 standard deviation of total ammonia concentration in the wastewater treatment plant effluent
80 to reflect the stability of the treatment process, but only to reflect the variation in total ammonia
81 concentration within a time series for different operational scenarios. Mohammadiun et al.
82 (2018) implemented a stochastic formulation for the design of urban drainage systems using

83 blockage probability and probability of the failure, as the measure of resilience under stochastic
84 conditions. However their approach only uses probability estimates and does not capture
85 detailed information on uncertainty. Similarly, Yu et al. (2017) applied a stochastic
86 optimization model for urban drainage design by applying chance constrained programming.
87 The uncertainty arising from the simulation models is handled by limiting the total surcharge
88 volume to an acceptable value by specifying a risk level as probability value. Zhang et al.
89 (2019) applied a surrogate model based optimization to aid design for urban flood mitigation.
90 They accounted for uncertainty arising from surrogate models and compared the surrogate
91 model based optimization results to results from a 2D dynamic flood model using different
92 rainfall scenarios. Lin et al. (2020) implemented a multi-objective optimization based design
93 of urban drainage systems for protection against flooding. In order to make the design resilient
94 against future uncertainties, they minimized the standard deviation of the maximum water
95 depths in pipes. Similar to the studies mentioned before the representation of uncertainty by
96 the use of standard deviation does not account for any asymmetry or the extremes of the
97 distribution of predicted performance.

98 The probability of exceeding a threshold only indicates the chance that this threshold will be
99 exceeded, however, it does not provide any information about the magnitude of the exceedance
100 beyond the threshold. Studies such as Moreno-Rodenas et al. (2019) and Rico-Ramirez et al.
101 (2015) have shown that the uncertainty in sewer system simulation outputs were generally
102 found to have asymmetrical distributions. In the case of CSO spills, the environmental impact
103 not only depends on the number of CSO spill events but also on the size and duration of each
104 failure and the pollutant concentration and loads released. The authors argue that in this field a
105 decision maker is likely to prefer asymmetry in a system's performance. The preference for
106 asymmetry relates to the sensitivity of the receiving water body. A receiving water body highly
107 sensitive to incoming pollutant loads may drive the decision maker to prefer a negatively

108 skewed distribution which does not have a long tail of rare but impactful events. A less risk-
109 averse individual, however, may accept a small chance of a high negative impact in order to
110 reduce the overall risk of failure.

111 Unlike existing studies, this paper fully utilizes the information provided by the uncertainty
112 quantification process by including information on skewness and the magnitude of the tail of a
113 probability distribution of a system performance measure. In doing so, this paper aims to
114 develop a new decision-making approach, which accounts for decision makers' risk
115 preferences using information on uncertainty in the sewer system's predicted performance.

116 In this new approach, the decision model uses a multi-objective formulation to reflect both the
117 decision maker's objectives as well as his/her risk-averseness. As far as the authors are aware,
118 the inclusion of risk preferences when accounting for uncertainty in making decisions for the
119 management of intermittent CSO spills has not been reported before, and can have considerable
120 implications for investment costs. Key contributions of this paper are: (i) identifying the
121 characteristics of probability distributions to represent the risk preference of the decision
122 maker, and (ii) analysing the implications of the risk preference of the decision maker on the
123 investment decisions in the presence of conflicting objectives using uncertain system
124 performance predictions.

125 The proposed decision-making approach is demonstrated using data from a case study
126 catchment located in the North-West of Luxembourg.

127

128

129 **2. Background and Methodology**

130 **2.1. Background**

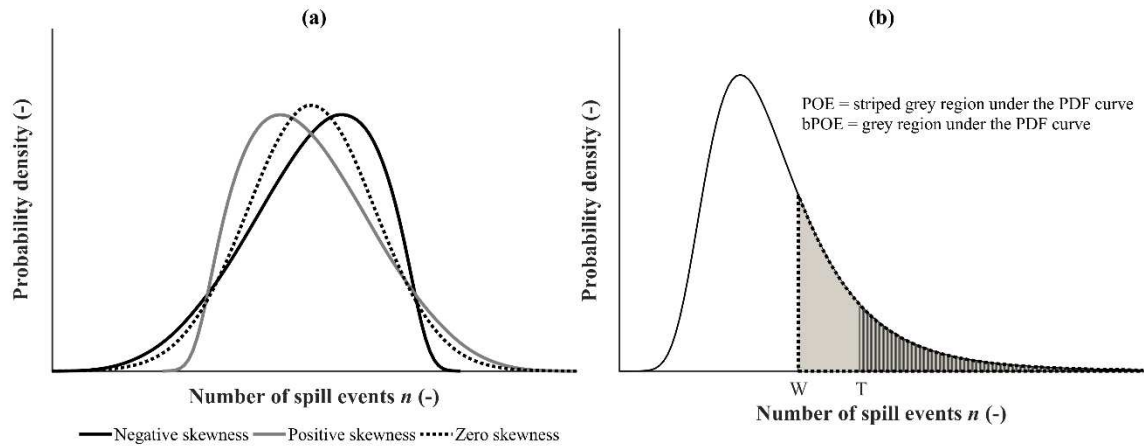
131 One of the most popular approaches for risk-averse decision-making has been the mean-
132 variance approach developed by Markowitz (1952) for investment portfolio selection in the
133 field of finance. This approach assumes that variance of the rate of return can be used as a
134 measure of risk and that the decision maker should search for a selection with minimum
135 variance for an expected rate of return on investment. In the context of this study, the desired
136 decision criterion can be translated to a minimum variance for a given expected number of
137 CSO spill events above a regulatory threshold. A bi-objective decision problem can be
138 formulated to search for solutions which result in minimum mean and minimum variance of
139 the number of predicted spill events. However, the mean-variance approach has certain
140 limitations. It assumes that statistical distributions are Gaussian and that minimising variance
141 penalizes distributions equally at both tails. For CSO spill events, the number of failures is
142 usually defined as a threshold to the number of events (n) exceeding an allowed number of
143 CSO spills in a defined time period, or a threshold exceeding an allowed number of events
144 which are causing one or more water quality indicators to exceed a regulatory limit (for
145 example, duration high ammonia concentration levels in the receiving water). As the method
146 works for any threshold, a threshold is defined simply as 'T'. Hence, the decision maker would
147 desire to limit the spread only on the right side of the probability distribution of n , i.e. to limit
148 high values of n because only values of n greater than the threshold T would result in a breach
149 of the regulatory requirements.

150 The issue of non-normal distributions can be dealt with by considering the skewness of the
151 distribution as one of the decision criteria such as adopted in the Mean-Variance-Skewness
152 approach proposed by Konno and Suzuki (1995) for investment portfolio selection. Konno and
153 Suzuki (1995) argued that skewness of the distributions had a significant influence on the
154 optimal selection of decision alternatives and proposed that the decision maker should prefer
155 to maximise the skewness to optimise the rate of return on investment. However, unlike the

156 rate of return on financial investments, the reasoning for the decision maker's preference to
157 maximise skewness may not be so apparent for CSO spill events that cause regulatory failure.
158 It can be argued that both types of asymmetry have distinct strengths and weaknesses in the
159 context of managing water quality failure caused by intermittent CSO spills. For example, a
160 small probability of a large number of spills may not be very significant when regulations only
161 focus on a number of spills, and/or because these spills may be small in size. However, if the
162 regulations are related to receiving water quality parameters and/or volume of spills, a small
163 chance of a single huge event that destroys particular species of aquatic life in the receiving
164 water could be a significant concern.

165 A positively skewed distribution (Fig 1a) will have a lower mode compared to a negatively
166 skewed distribution, which means the most likely realizations of spill events n will be less than
167 that of a negatively skewed distribution. Therefore, a decision maker who is more concerned
168 about the most likely value of the number of CSO spill events and is prepared to absorb the
169 small chance of high values of n (i.e. a long tail of the distribution of n), would prefer a
170 positively skewed distribution. On the contrary, a decision maker who seeks to limit the
171 possibility of very high values of n would prefer a negatively skewed distribution. Such a
172 decision maker can be considered more risk-averse because their goal is to seek protection
173 against the occurrence of very high number of CSO spills (i.e. avoiding long right tail) rather
174 than limiting the most likely number of spill events.

175



176

177 Fig. 1. (a) Difference in skewness for distributions with identical mean and variance. (b) Illustration of
 178 Probability of Exceedance and Buffered Probability of Exceedance for a threshold T on the number of spill
 179 events n .

180 Considering variance as a measure of risk in the Mean-Variance-Skewness approach does not
 181 address the risk of exceeding a threshold T imposed by environmental regulations. The
 182 probability of failing this set criterion can be calculated as the Probability of Exceedance
 183 (POE). If n is a random variable representing the number of CSO spill events and T is the
 184 threshold set to determine CSO emission failure, POE for threshold T can be defined as

$$\text{POE}(n) = P(n > T) \quad (1)$$

185 However, the POE and the threshold T do not fully describe the shape of heavy-tailed
 186 distributions, they do not provide any information on the magnitude of n in the tail beyond
 187 threshold T . Uryasev (2014) proposed a measure called the Buffered Probability of Exceedance
 188 (bPOE) to reflect the magnitude of the probability in the tail beyond the threshold T . The POE
 189 gives the likelihood that the threshold T will be exceeded whereas, the bPOE gives the
 190 likelihood that the average of the distribution's upper tail will be equal to the threshold T (Davis
 191 and Uryasev, 2016). Consider a quantity W in the uncertain range of n such that $T = E[n|n >$
 192 $W]$, where $E[n|n > W]$ is the conditional expectation of the number of spill events n exceeding

193 W (Fig. 1b). From Mafusalov and Uryasev (2014) and, Davis and Uryasev (2016), the bPOE
194 for threshold T can be defined as:

$$\text{bPOE}(n) = P[n > W] \quad (2)$$

195 Since, $T \geq W$, there exists an inequality between bPOE and POE which can be expressed as,

$$\text{POE}(n) \leq \text{bPOE}(n) \quad (3)$$

196 The inequality in (3) implies that the bPOE is a conservative estimate of the POE because it
197 accounts for the magnitude of the tail in addition to the probability (Fig. 1b). Hence, it will be
198 a better measure than the POE if the decision maker is risk-averse and is interested in
199 comparing the tail performance of the distribution of the number of CSO spills for modelled
200 engineering interventions to limit the occurrence of CSO emission failure.

201

202 **2.2. Methodology**

203 Building on the previous arguments, a decision model is proposed where the decision maker is
204 seeking to minimize the risk of non-compliance with environmental regulations while
205 minimizing the intervention cost. The proposed decision model has four objectives: (i)
206 Minimizing the expected value of the number of CSO spill events $E[n]$; (ii) Minimizing the
207 bPOE for a defined threshold on the number of CSO spill events; (iii) Maximizing or
208 Minimizing the skewness of the distribution of n ; and (iv) Minimizing the cost of any proposed
209 engineering intervention.

210 Since the preference for the shape of the distribution (objective iii) is specific to this application
211 and an individual's risk behaviour, two versions of the decision model (D1 and D2) are
212 proposed to reflect the differing preferences for the skewness in the context of managing the
213 impact of CSO emission failures. Since the decision models D1 and D2 seek solutions which

214 minimise the bPOE value which is an indicator of risk, both D1 and D2 can be considered as
 215 risk-averse decision models.

216 **2.2.1. Formulation of the multi-objective decision model**

217 This section presents the mathematical formulation of the proposed risk-averse decision model.
 218 Consider a quantity $n = f(s, u)$ which represents the performance of a combined sewer system
 219 model with decision variables $s \in S$ where S is the decision space, and uncertain inputs and
 220 parameters $u \in U$. Let us assume that uncertain inputs and parameters u represent the
 221 uncertainty in the modelling of the sewer system performance n defined on the uncertainty
 222 space U . For a given $s \in S$, uncertain inputs and parameters u will result into random
 223 realizations of the quantity of interest n which can be represented by $n_s = f_s(s, u)$.

224 Two risk-averse decision models D1 and D2, are posed as multi-objective problems:

$$D1 : \begin{cases} \min_{s \in S} E[f_s(s, u)] \\ \min_{s \in S} \text{bPOE}(f_s(s, u)) \\ \max_{s \in S} \text{skewness}(f_s(s, u)) \\ \min_{s \in S} \text{cost}(s) \end{cases} \quad (4)$$

$$D2 : \begin{cases} \min_{s \in S} E[f_s(s, u)] \\ \min_{s \in S} \text{bPOE}(f_s(s, u)) \\ \min_{s \in S} \text{skewness}(f_s(s, u)) \\ \min_{s \in S} \text{cost}(s) \end{cases} \quad (5)$$

subject to $u \in U$

225 A decision maker may have biased i.e. have unequal preferences for the individual objectives;
 226 however, the objectives in D1 and D2 are treated as equally preferable to each other.
 227 Consequently, the decision maker may apply their preferences for the objectives *a posteriori*.

228 **2.2.2. Pareto Non-dominance**

229 The multi-objective formulation of D1 or D2 will not necessarily lead to a single optimal
230 solution due to the conflicting nature of the objectives. Hence, the decision model searches for
231 non-dominated solutions in the decision space S . The dominance of one solution to the other is
232 established by determining the Pareto optimality of the decision variables in the decision space
233 S against the individual objectives. A Pareto optimal solution can be defined as the solution for
234 which improvement of one objective is not possible without worsening at least one of the other
235 objectives. The dominance of one solution to the other can be defined as follows:

236 For two solutions s^1 and $s^2 \in S$, s^1 dominates s^2 if and only if

$$s_i^1 \geq s_i^2 \quad \forall i \tag{6}$$

and $s_i^1 > s_i^2$ for at least one objective in i

237 where i is the set of objectives.

238 Therefore, a solution s^* is Pareto optimal such that there exists no $s \in S$ which satisfies the
239 following inequalities:

$$s_i^* \geq s_i \quad \forall i \tag{7}$$

and $s_i^* > s_i$ for at least one objective in i

240 Solving the multi-objective decision problem D1 or D2 by searching for non-dominated
241 solutions as per Eq. 6 and 7 will result in a set of Pareto optimal solutions s^* . The approach is
242 illustrated using a case study.

243

244

245 **3. Case Study: The Haute-Sûre Catchment in Luxembourg**

246 The case study catchment is part of the Haute-Sûre catchment located in the North-West of
247 Luxembourg. The case study catchment has a combined sewer system, serving the urban area
248 of Goesdrof with a single CSO structure composed of a storage tank and a weir to divert excess
249 flows during intense rainfall events towards a tributary of the Sûre river. The CSO structure
250 currently has a storage volume of 190 m³ and the case study catchment size is 36 ha with an
251 impervious area of 25 ha. This catchment is selected because the receiving water body is
252 considered sensitive to the high ammonium and ammonia concentrations and thus exhibits
253 aspects common in many situations in which investment may be required to better manage
254 intermittent discharges in line with regulatory requirements. Further details of the case study
255 catchment are given in Torres-Matallana et al., (2018)

256

257 **3.1. Compliance with the environmental regulations**

258 The uncertainty of the predicted ammonium concentration in the CSO emission is estimated
259 and applied in the risk-averse decision model to find solutions which reduce the risk of
260 regulatory failure caused by ammonium in the sewer overflows and also attempt to minimise
261 cost. The concentration-duration-frequency based criterion used as a compliance tests was
262 originally specified by the Austrian water wastewater association (ÖWAV) for receiving
263 surface waters and is applied in this case study as an indicative emission quality standard
264 (ÖWAV-Regelblatt 19, 2007), This standard is more restrictive than standards defined in
265 several other European countries. The criterion for acute ammonia toxicity comprises separate
266 thresholds for cyprinid and salmonid aquatic species. According to the ÖWAV guidelines, the
267 maximum allowable number of CSO spill events failing this criterion for acute ammonia
268 toxicity is 1 per year. This case study applies a dilution ratio to the predicted CSO spill
269 ammonium concentration in order to account for the reasonably expected dilution of the CSO
270 spill with the receiving water body. Morgan et al. (2017) list a range of dilution ratios which

271 indicate the significance of stormwater overflows (SWO) to different types of receiving water
272 bodies. They report a dilution ratio < 2:1 for SWOs with high significance, between 2:1 and
273 8:1 for medium significance while dilution ratio would be in the upwards of 8:1 for SWOs with
274 low significance. For the purpose of demonstrating the decision methodology, this paper uses
275 a value of 4 as a reasonable indicative dilution ratio for representing the dilution of CSO spills
276 by flows in receiving waters.

277

278 **3.2. The EmiStatR model**

279 The performance of proposed solutions is evaluated using an open-source CSO water quality
280 simulator EmiStatR, This scalable and highly computationally efficient simulator had been
281 specifically developed to obtain water quantity and quality predictions with a similar level of
282 accuracy compared to the results from complex mechanistic hydrodynamic models, such as
283 InfoWorks. Its computationally efficiency made it ideal for studies in which computationally
284 intense Monte Carlo based approaches were used to quantify the impact of uncertainty..
285 EmiStatR has therefore been used in earlier studies that investigated the propagation of input
286 and model parameter uncertainties in the simulation of NH₄-N concentration in CSO spills
287 (Torres-Matallana et al., 2018). The EmiStatR simulator uses six main components to simulate
288 CSO spill quantity and quality: (i) Computation of dry weather flow; (ii) Definition of water
289 quality characteristics of the dry weather flow; (iii) Computation of wet weather flow in the
290 sewer network with contributions from urban and rural runoff; (iv) Definition of water quality
291 characteristics of urban and rural wash-off; (v) Computation of combined sewage flow and
292 characteristics of water quality variables in the combined sewage flow; and (vi) Computation
293 of CSO spill volume and NH₄-N concentration and load.

294 A comprehensive description of the EmiStatR model can be found in Torres-Matallana et al.
295 (2018) including the model calibration and validation approaches. The hydraulic calibration
296 data set, contained three rainfall/spill events and consisted of detailed precipitation and CSO
297 water level observations from 15 May 2011 to 3 June 2011 with the temporal resolution
298 aggregated to 10 min to ensure identical temporal resolution in simulated and observed data.
299 The DiffeRential Evolution Adaptive Metropolis (DREAM) algorithm (Vrugt et al., 2009) was
300 used for calibration. The calibrated model displayed good agreement with the CSO water level
301 observations in the calibration data set with a Nash-Sutcliffe Efficiency, NSE of 0.95.

302 The hydraulically calibrated EmiStatR model was validated using observations of precipitation
303 and water level at the CSO storage chamber, at aggregated 10 minute intervals containing nine
304 rainfall/spill events collected from 3 June 2011 to 7 July 2011. The EmiStatR model displayed
305 a reasonable agreement (NSE = 0.78) with the observations in the validation data set.
306 Additional validation of the hydraulic performance of the calibrated EmiStatR model included
307 a comparison against a detailed hydrodynamic sewer network model of the catchment built and
308 calibrated using InfoWorks ICM 7.5 covering an entire year (2010) at 10 minutes resolution,
309 including 16 CSO spill events. For this validation period, the EmiStatR simulations of CSO
310 volume displayed good agreement (NSE = 0.79) with the InfoWorks ICM model. This suggests
311 that the EmiStatR can be used as a suitable rapid hydrodynamic simulation tool to demonstrate
312 the proposed decision-making approach, with the advantage that EmiStatR is deployed as a
313 scalable parallel simulator that allows multi-core simulation with a lower computational
314 demand when it is compared to a detailed hydrodynamic sewer network model.

315 In the absence of water quality observations in CSO spills, the EmiStatR was further validated
316 against water quality predictions using the calibrated InfoWorks ICM model for this catchment.
317 The comparison of EmiStatR and InfoWorks ICM hydraulic and water quality simulations
318 were done using a 1 year-long rainfall timeseries with 10-minute resolution. A good agreement

319 was found between the EmiStatR and the InfoWorks ICM model for simulating CSO spill
320 volume (NSE = 0.78) and ammonium load (NSE = 0.82).

321 **3.2.1. Decision variables**

322 To limit the number of CSO spill events failing the criterion defined in section 3.1, two types
323 of solutions are considered: changing the storage capacity of the tank at the CSO and a
324 reduction in impervious area through the provision of permeable paving to replace
325 impermeable surfaces (Table 1). Combinations of solutions are then modelled and evaluated
326 against emission failure criterion and cost. For storage tank capacity, 4 values: 100 m³, 500 m³,
327 900 m³ and 1700 m³ have been selected. These values have been selected as such to enable the
328 evaluation of the performance of storage volume over a range that is expected to show a wide
329 range of failures relative to regulatory requirements. This case study evaluates the decision
330 model at impervious area values 20 ha, 23 ha and 25 ha. Similar to the selected range for storage
331 tank capacity, a limited, but reasonable range of impervious area reduction from 25 ha to 20 ha
332 was used. These choices for the decision space are specific to this case study.

333 **3.2.2. Cost of the decision variable s**

334 Detailed information about the capital cost of storage tanks and permeable paving is not
335 available for Luxembourg, estimates from the UK are therefore used in this study. The
336 construction of storage tanks can cost in the range of £1,400 - £2,000/m³ for areas outside
337 London whereas the implementation of permeable paving can cost approximately from £250 -
338 £350/m² (Digman, 2018). Costs can vary depending on the construction company and
339 catchment characteristics, such as location, property values and urban density. Fixed average
340 values of solution costs i.e. £1,700/m³ for the storage tank and £300/m² for the permeable
341 paving have been used in this study to estimate the cost of the decision variable *s*, as the quality
342 of the cost data provided did not allow a robust estimate of cost uncertainty to be made. No

343 uncertainty is considered for the cost estimate for any solution, this was deemed reasonable
344 given the quality of the cost data and that the main aim of the study was to examine the
345 influence of predictive model uncertainty on risk perception.

346 **3.2.3. Definition of uncertain inputs and parameters**

347 Table 1 presents the list of inputs and parameters that could be considered uncertain for the
348 Goesdorf sewer system. The list contains all the input parameters for which data was available
349 to characterise uncertainty in their estimates. Measured data to characterise any temporal
350 variability of the ammonium concentration in the surface runoff for this catchment is not
351 available. Hence, uncertainty in this variable for this catchment could not be quantified and
352 accounted for. Welker (2007) reported the ammonium concentration in surface runoff to be at
353 1mg/l as a representative value for a catchment in Germany following an extensive literature
354 survey of pollutant concentrations in surface runoff. In the absence of more information on
355 ammonium concentration in surface runoff for a catchment in Luxembourg, this paper uses the
356 value of 1mg/l which could be considered suitable for a European catchment subject to similar
357 farming regulations and practices.

358 Before the uncertainty propagation, probability distribution functions of the selected inputs are
359 characterised to define the input uncertainty (Heuvelink et al., 2007). For the concentration of
360 ammonium in the wastewater flow $C_{NH_4,s}$ as a variable for uncertainty propagation, it is possible
361 to simulate $C_{NH_4,s}$ by an autoregressive order one AR(1) model (Box & Jenkins, 2008):

$$y_t = \mu_1 + \varphi_1(y_{t-1} - \mu_1) + w_t, \quad \varphi_1 \neq 0 \quad (8)$$

362 where y = Univariate variable $C_{NH_4,s}$; t = Time; μ_1 = Mean of the simulated variable; φ_1 =
363 Constant coefficient of autocorrelation; w_t = Gaussian white noise time series with mean zero
364 and variance σ_w^2 .

365

366 **Table 1. List of uncertain and decision variables.**

| Variable | Assumed to be uncertain? (yes/no) | Definition of uncertainty |
|---|--------------------------------------|--|
| Uncertain Inputs and Parameters | | |
| <i>Wastewater – Dry Weather</i> | | |
| Pollution NH ₄ -N, $C_{NH_4,s}$ [g/(PE·d)] | yes | Autoregressive model ^a calibrated on measured data |
| <i>Rainwater</i> | | |
| Precipitation time series, P [mm/Δt] | yes | Multivariate Autoregressive model ^b calibrated on measured data |
| <i>Catchment data</i> | | |
| Runoff coefficient for impervious area, C_{imp} [-] | yes | N(0.8, 0.05) truncated at 0 and 1 ^c |
| Runoff coefficient for pervious area, C_{per} [-] | yes | N(0.3, 0.05) truncated at 0 and 1 ^c |
| Decision Variables | | |
| <i>Catchment data</i> | | |
| Impervious area, A_{imp} [ha] | no | - |
| <i>CSO structure data</i> | | |
| Volume, V [m ³] | no | - |

367 ^aBox et al. (2008), ^bTorres-Matallana, et al. (2017), ^cMcCuen (1998).

368 This paper uses the available rainfall precipitation measurements from the Esch-sur-Sûre rain
369 gauge which is located around 3.5 km away from the Goesdorf CSO structure. The rainfall
370 time series has a resolution of 10 minutes and contains 10 year-long precipitation
371 measurements from January 2010 until December 2019. Since the rainfall precipitation time
372 series contains many zero values, a different approach for characterising uncertainty in the
373 rainfall time series has to be applied. A multivariate autoregressive modelling and conditional
374 simulation of precipitation time series from Torres-Matallana et al. (2017) is used to simulate
375 precipitation time series in the Goesdorf catchment given a measured precipitation time series
376 in a nearby location outside the catchment while accounting for the uncertainty that is
377 introduced due to spatial and temporal variation in precipitation. The inherent uncertainty in
378 the measured rainfall is considered as a function of two neighbouring stations to assess the
379 uncertainty i.e. Dahl and Esch-sur-Sure rainfall stations are used to define the rainfall time

380 series at Goesdorf catchment while accounting for uncertainty. Torres-Matallana et al. (2017)
381 note that their method does not capture the distribution tails well and in a small number of
382 cases, results in an overestimation of the simulated precipitation.

383 McCuen (1998) reported an indicative range of 0.25-0.40 for the runoff coefficient of pervious
384 surfaces and a range of 0.70-0.95 for impervious surfaces. Since the runoff process from the
385 catchment surfaces is a natural process, a symmetrical normal distribution is assumed to
386 represent the uncertainty in the runoff coefficients. Table 1 indicates the normal distributions
387 selected, such that about 95% of the runoff coefficient values lie in these ranges.

388

389 **3.3. Solving the decision model**

390 The decision space S in the current case study is discrete and finite, and comprises 12 grid
391 points (s) for each decision model. In this case, the objective functions are evaluated at each
392 grid point covering the decision space.

393 Fig. 2 outlines the steps involved in identifying the Pareto optimal solutions for the decision
394 models D1 and D2. To evaluate the objectives in Eq. (4) or (5), for each of the 12 grid points
395 in the decision space S , $n_s = f_s(s, u)$ is calculated where n_s is the emission quality indicator, s
396 is the grid point representing decision variable and u is the uncertainty defined in section 3.2.3.
397 For each $s \in S$ the uncertainty u in the inputs and model parameters listed in Table 1 are
398 propagated through 500 Monte Carlo simulation runs for a 10 year period. The number of runs
399 was selected after a convergence test that demonstrates this number as suitable to perform
400 Monte Carlo simulations. For the simulation outputs CSO volume and ammonium
401 concentration, standard deviation of the output variables at each time step from two different
402 Monte Carlo simulations with different seed for the pseudo-number generator algorithm was

403 compared. Convergence tests indicated 500 Monte Carlo simulations are sufficient to obtain
404 consistent results ($NSE \approx 0.999$ for CSO volume and $NSE \approx 0.998$ for NH_4-N concentration).

405 These Monte Carlo simulations result in 500 random samples of 10 year-long time series of
406 NH_4-N concentration in the CSO spill. According to ÖWAV guidelines, during 1 year the
407 concentration of ammonia in the receiving water body due to a combined sewer overflow
408 should not be more than 5 mg/l for one hour for cyprinid species (ÖWAV-Regelblatt 19, 2007).

409 As per the criterion whenever the concentration of ammonia exceeds the threshold for an hour
410 or more, it is counted as one failing CSO spill event. Two consecutive events are separated
411 whenever, the concentration of ammonia drops below the threshold concentration. After
412 multiplying with a dilution ratio of 4:1, this emission failure criterion is applied to the simulated
413 NH_4-N concentration time series to calculate the number of non-compliant CSO spill events
414 for every random time series. This results in 500 random samples of the emission quality
415 indicator n_s for each $s \in S$.

416 Individual objective functions of the decision models are calculated using the random samples
417 of $n_s \forall s \in S$. The decision variables s are compared to each other for Pareto non-dominance by
418 using inequality Eq. (6). All the grid points which satisfy the inequality Eq. (7) are selected as
419 Pareto optimal solutions which represent the optimal trade-off between the individual
420 objectives (Minimising mean of n_s ; Maximising or Minimising skewness of n_s ; Minimising
421 bPOE, and; Minimising cost of s) set by the decision maker in D1 and D2.

422

Step 1: Define

- Emission quality indicator n_s : Number of CSO spills with $\text{NH}_4\text{-N}$ concentration $> (5 \times \text{dilution ratio}) \text{ mg/l}$ for one hour
- Simulation output: $\text{NH}_4\text{-N}$ concentration in the CSO spills
- Decision variables $s \in S$ (Section 3.2.1)
- Cost of decision variables $s \in S$ (Section 3.2.2)
- Uncertain variables u (Section 3.2.3)
- Objective functions for the decision models D1 and D2 (Eq. 4 and 5)

Step 2: Propagate the uncertainty in u to simulate $\text{NH}_4\text{-N}$ concentration in the CSO spills $\forall s \in S$

Step 3: Estimate $n_s = f_s(s, u) \forall s \in S$ by identifying spill events with $\text{NH}_4\text{-N}$ concentration $> (5 \times \text{dilution ratio}) \text{ mg/l}$ for one hour, during 1 year on average

Step 4: Compute the value of objective functions in D1 and D2 $\forall s \in S$

Step 5: Determine Pareto non-dominance relationship for D1 and D2 $\forall s \in S$ (Eq.7)

Step 6: Identify Pareto optimal solutions for the decision models D1 and D2

423

424 Fig. 2. Steps followed to identify Pareto optimal solutions for D1 and D2.

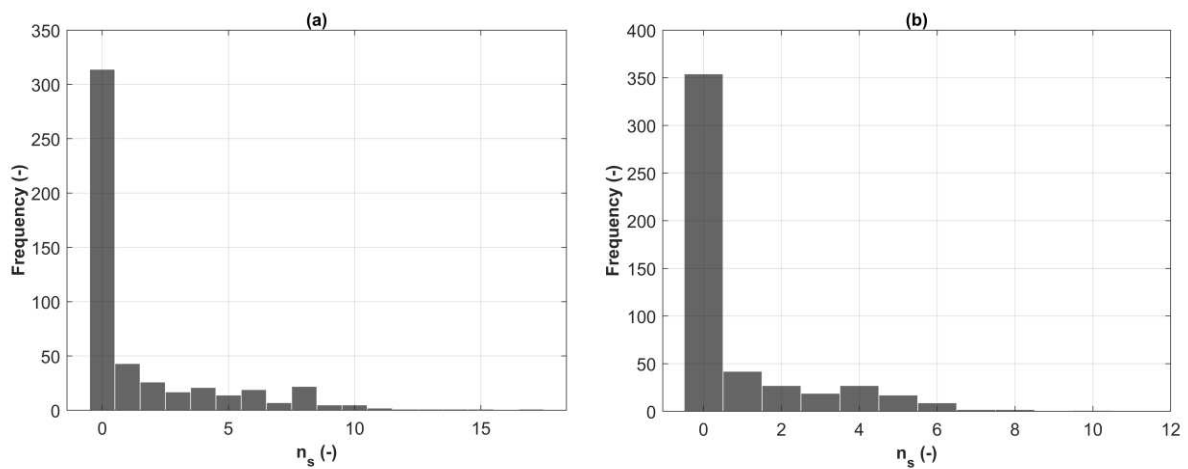
425 It can be argued that it would be computationally more efficient to deterministically optimize
426 the system for cost and number of critical spills without considering model predictive
427 uncertainties then carry out MC simulations only for the non-dominated solutions and calculate
428 bPOE and skewness only for these solutions. However, the Pareto optimality or non-dominance
429 of solutions will change when model predictive uncertainty is considered, therefore, any
430 solution deemed non-dominated or Pareto optimal based on a deterministic performance
431 indicator is unlikely to be non-dominated if model predictive uncertainty is considered and this
432 difference justifies the use of the more computationally expensive approach.

433

434

435 **4. Results and Discussion**

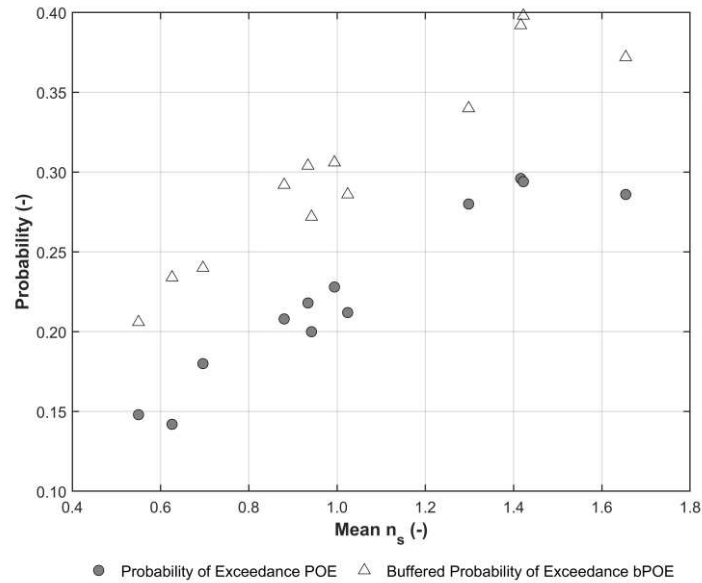
436 The decision models D1 and D2 are evaluated for the case study presented in Section 3 with
437 decision variables s defined in Section 3.2.1 and, uncertain inputs and parameters u defined in
438 Section 3.2.3. Fig. 3 shows an example of the distribution of n_s in the form of a histogram for
439 the solution (900 m³; 23 ha). Fig. 3a and 3b demonstrate the skewness present in the distribution
440 of n_s .



441

442 Fig. 3. Histogram of n_s for the solutions: (a) (100 m³; 25 ha); (b) (900 m³; 23 ha)

443 Fig. 4 shows the difference in POE and bPOE for $\forall s \in S$. It is evident how the magnitude of
444 the tail values in the distribution of n_s affects the value of bPOE. The results for Pareto optimal
445 solutions are presented separately for the decision models D1 and D2 which reflect the different
446 preferences for the skewness of the distribution of n_s .



447

448 Fig. 4. Mean of n_s vs Probability of Exceedance (POE) and Buffered Probability of Exceedance (bPOE) for $\forall s$

449 $\in S$

450

451 **4.1. Decision model D1: Preference for positively skewed distributions of n_s**

452 For decision model D1, 10 solutions were found to be Pareto optimal or non-dominated out of

453 the 12 solutions (Fig. 5). Fig. 5a and 5b show the variation in the calculated mean of n_s and

454 bPOE respectively for all $s \in S$ where the decision variable s comprises combinations of storage

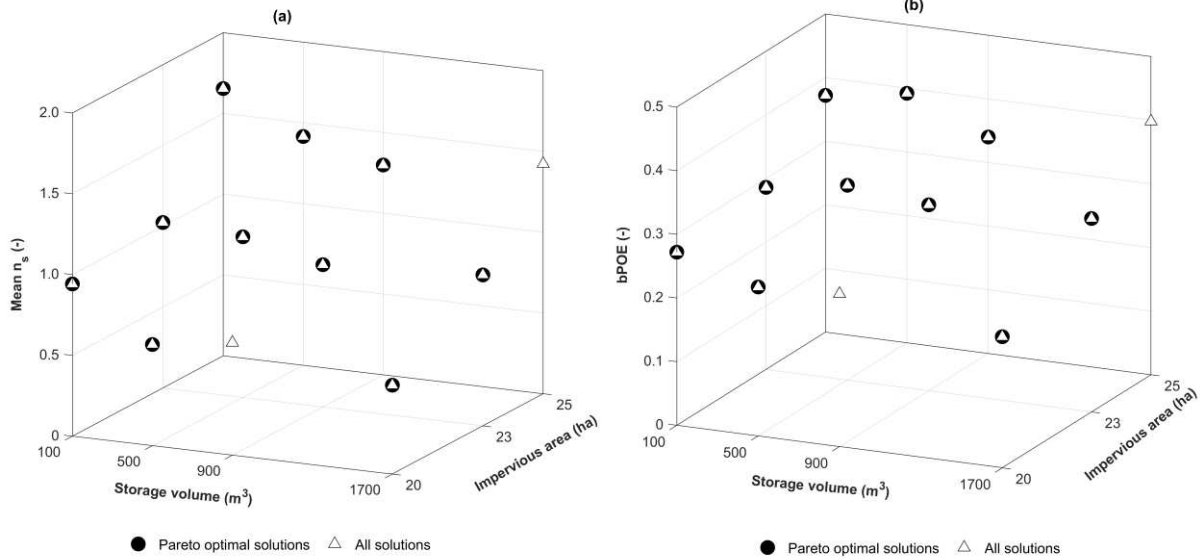
455 tank volume and impervious area. As expected, the mean of n_s decreases with an increase in

456 storage tank volume and/or a decrease in impervious area. The Pareto optimal solutions

457 representing the optimal trade-off between the four objectives (Minimising mean of n_s ;

458 Maximising skewness of n_s ; Minimising bPOE and Minimising cost of s) are displayed as data

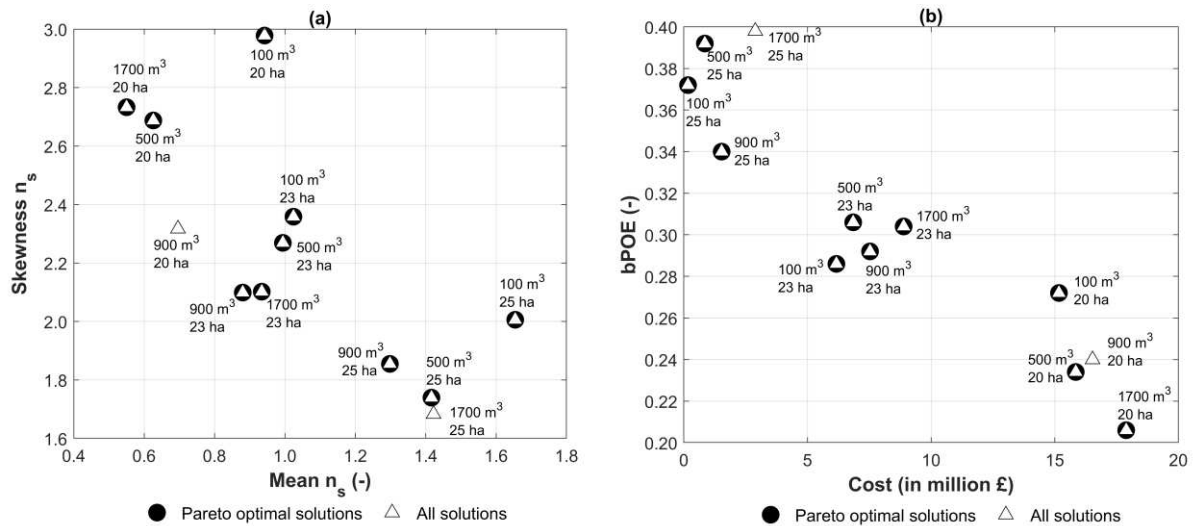
459 points in a solid black circle in Fig. 5.



460

461 Fig. 5. (a) D1: Mean of n_s in the discrete decision space S ; (b) D1: bPOE in the discrete decision space S

462 It can be observed that the decrease in the mean of n_s is steeper for a reduction in impervious
 463 area. For example, at the storage tank capacity of $900 m^3$, the mean n_s reduces from 1.3 to 0.7
 464 when the impervious area is reduced from 25 ha to 20 ha. On the contrary, at the impervious
 465 area of 20 ha, the mean reduces from 0.9 to 0.5 when the storage tank capacity is increased
 466 from $100 m^3$ to $1700 m^3$. A similar trend can be observed for bPOE values (Fig. 5b). Despite
 467 the considerably higher cost associated with impervious area reduction when compared to
 468 increasing the storage tank capacity, they are non-dominated solutions due to their better
 469 performance for the uncertainty related objectives.



470

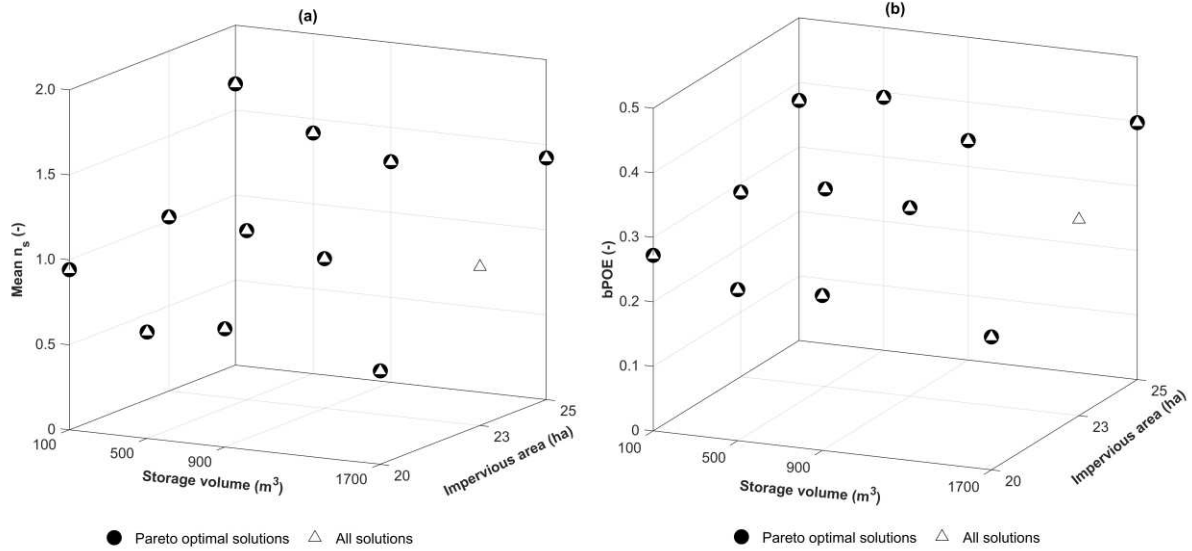
471 Fig. 6. (a) D1: Mean of n_s vs Skewness of n_s ; (b) D1: Cost of n_s vs Buffered Probability of Exceedance (bPOE)

472 Fig. 6a shows the variation in the mean of n_s vs the skewness of n_s . Fig. 6b shows the cost of
 473 the decision variables vs their respective bPOE values. Pareto optimal solutions would be
 474 expected to lie towards low cost and low bPOE values however there are a few Pareto solutions
 475 which have either very high cost and low bPOE or high value of bPOE and low cost. This can
 476 be attributed to an equal preference for all the objectives which means that these solutions must
 477 have performed well for the other objectives compared to the non-optimal solutions with
 478 similar cost or similar bPOE.

479

480 4.2. Decision model D2: Preference for negatively skewed distributions of n_s

481 For decision model D2, 11 solutions were found to be Pareto optimal out of 12 solutions (Fig.
 482 7). The only dominated or sub-optimal solution for D2 is (1700 m³; 23 ha) since D2 seeks to
 483 minimise the skewness value. The rest of the 11 solutions remain Pareto optimal due to their
 484 better performance in one or more objectives. The solution (1700 m³; 25 ha) performs worse
 485 for the mean, bPOE and the cost objective however it has the lowest skewness value which
 486 makes it non-dominated when one of the objectives is to minimise skewness.

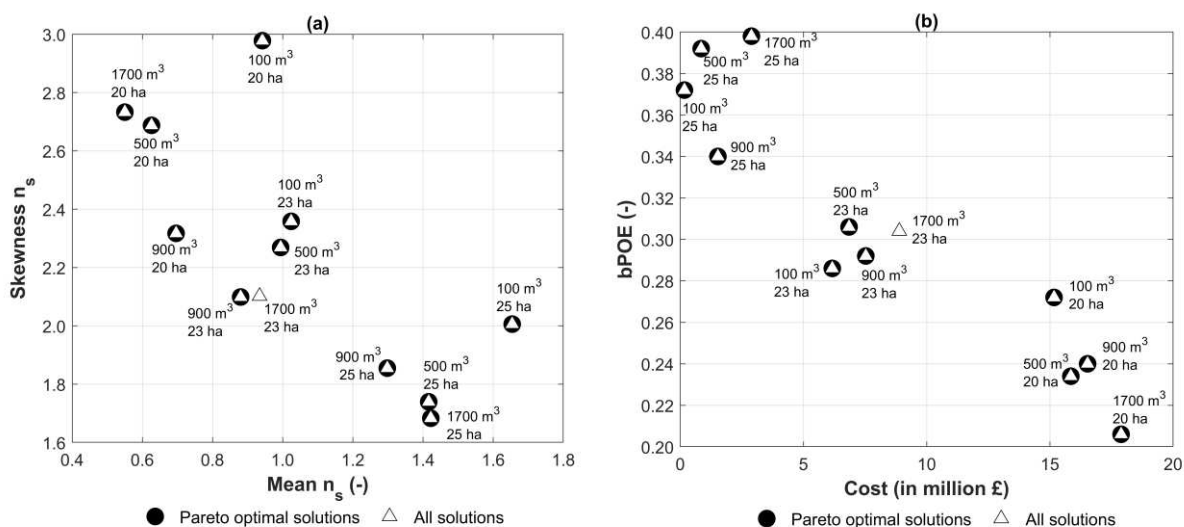


487

488 Fig. 7. (a) D2: Mean of n_s in the discrete decision space S ; (b) D2: bPOE in the discrete decision space S

489 This clearly demonstrates that how a poorer performing solution can become non-dominated
 490 with differing preferences of decision makers. Therefore, solutions which have a relatively high
 491 mean, are also Pareto optimal solutions because they satisfy the objective of minimizing the
 492 skewness to address desired risk preferences (Fig. 8a). However, this is more evident in Fig.
 493 8b where the Pareto optimal solutions for decision model D2 are displayed on the cost vs bPOE
 494 plot. Because of the decision maker's objective to minimize skewness, the Pareto non-
 495 dominance results in a diverse range of Pareto optimal solutions as far as only cost and bPOE
 496 are concerned. In such situations, preference for individual objectives needs to be updated to
 497 reflect the scope of the decision-making. For example, in this case study, the primary goal of
 498 the decision maker could be compliance with the environmental regulations while minimising
 499 the cost. Therefore, the Pareto optimal solutions which are closer to the lower-left region of
 500 Fig. 8b should represent the decision maker's updated preference for the decision model D2.

501



502

503 Fig. 8. (a) D2: Mean of n_s vs Skewness of n_s ; (b) D2: Cost of n_s vs Buffered Probability of Exceedance bPOE

504 The decision models D1 and D2 provide the flexibility of representing other criteria in addition
505 to the modelled system performance and cost; the decision model can be scaled up to include
506 such criteria as objectives or constraints.

507

508 4.3. Implications of risk preferences on investment decisions

509 The proposed decision-making approach incorporates the uncertainty information in the
510 predicted CSO's performance variable n_s through three objective parameters: mean n_s , bPOE
511 and skewness of the distribution of n_s , with the cost added as a fourth objective parameter. The
512 goal of the decision-making process is to minimise the mean and bPOE values. Different
513 decision makers may exhibit varying degrees of risk aversion to regulatory failure and this can
514 be accounted for in the value of the skewness of the n_s distribution and the bPOE among the
515 four objectives in selecting their preferred solution. As a result, the selected investment at the
516 end of the decision-making process can be greatly influenced by the individual risk aversion
517 level of the decision maker, as illustrated by an example based on the case study outputs, as

518 shown in Table 2. Consider an example, in which a certain value of the mean of the CSO's
 519 performance variable n_s are desired, and in each case, the financial impact of the risk aversion
 520 level of the decision maker as represented by the skewness is shown.

521 **Table 2. Illustrative investment decisions for different asymmetry preference.**

| | Investment solution | Mean n_s | Cost |
|---------------------|-----------------------------|------------|--------------|
| Example | | | |
| Minimising skewness | 1700 m ³ ; 23 ha | 0.93 | £ 8,890,000 |
| Maximising skewness | 100 m ³ ; 20 ha | 0.94 | £ 15,170,000 |

522

523 Table 2 lists an illustrative example of comparing solutions with different preferences for
 524 skewness. In this example, the average protection, i.e. mean of n_s is kept at a very similar level.
 525 If the decision-maker prefers maximising the skewness, to achieve the same protection level as
 526 someone who prefers minimising skewness, the amount of investment required would be
 527 approximately two times higher. It should be noted here that maximising skewness may not
 528 always result in more expensive solutions when trying to achieve similar protection levels.
 529 These observations are specific to this case study example only. The example illustrates the
 530 potential for significant financial impact on a water utility, which is looking to meet the
 531 regulatory requirements but does not have a consistent risk acceptance or preference policy
 532 within its organisation to moderate the risk preferences of individual decision makers.

533 Similarly, two solutions can have identical values of POE but different values of bPOE
 534 indicating different tail magnitudes. Table 3 lists an example for illustrating the impact of tail
 535 magnitudes on an investment solution's performance. It is evident that the solution (900 m³;
 536 25 ha) is better than the solution (100 m³; 25 ha) based on bPOE value meaning the tail of (100
 537 m³; 25 ha) has higher magnitude.

538

539 **Table 3. Impact of the magnitude of tails in the distribution.**

| Investment solution | POE | bPOE |
|----------------------------|------|------|
| Example | | |
| 100 m ³ ; 25 ha | 0.28 | 0.37 |
| 900 m ³ ; 25 ha | 0.28 | 0.34 |

540

541 However, if the decision maker were to compare both the solutions only based on their POE
542 value, they would assess them as equivalent in performance.

543

544

545 **5. Conclusion**

546 Uncertainties in the simulation of the performance of urban sewer systems pose challenges to
547 decision makers in managing the environmental impact of intermittent sewer overflows. This
548 paper presents a rigorous risk-averse decision-making approach, which incorporates detailed
549 information on the shape of the probability distribution in the simulation of the performance of
550 solutions. The decision model consists of a trade-off between three objectives representing
551 uncertainty in the system performance, with the cost of the proposed solutions as the fourth
552 objective.

553 Using low-order statistical moments (mean or variance) or using the probability of exceedance
554 as a failure probability does not provide any information about the shape of the non-normal
555 probability distribution or the magnitude of the tails of the distributions that describe the system
556 performance in relation to regulatory thresholds. In this paper, the inclusion of skewness and
557 bPOE as objectives enables the decision maker to compare solutions against the symmetry and
558 tail characteristics of their uncertain performance explicitly.

559 Compared to the existing literature on managing sewer overflow impact, the proposed decision-
560 making approach provides decision makers with the flexibility to express their preferences for
561 risk averseness. Decision makers can find solutions satisfying their preference by analysing the
562 shape of the regulatory failure distribution and the level of risk acceptance under known budget
563 constraints. The case study illustrated that utilising a rigorous decision-making approach would
564 probably lead to considerably different investment solutions compared to approaches that do
565 not account for the level of risk-averseness of decision makers. This shows the importance of
566 taking into account uncertainty as well as the shape of the probability distribution of the
567 regulatory performance indicator. The case study clearly illustrated that the level of risk
568 averseness of an individual or a team in an organisation would have a considerable impact on
569 any investment decision, and that this impact is of a same order of magnitude as the impact due
570 to uncertainty in the predictive model parameters. Differing risk preferences could result in a
571 selection of investment solutions which cost substantially more or less for comparable values
572 of mean or POE failure performance.

573 This means that within the organisation of a water utility, a considerable difference in the cost
574 of approved regulatory compliant engineering solutions can be obtained owing to risk
575 preference of individuals or small teams within an organisation. These differences in
576 individuals' risk preferences have an impact of the same order of magnitude as the impact of
577 uncertainty in the predictive model parameters. To reduce the impact of different risk
578 preferences on individual investment decisions it is recommended to define a consistent
579 corporate risk preference policy within a water utility. Internationally there are a number of
580 regulatory frameworks (e.g. Water Framework Directive, NPDES CSO Control Policy,
581 (USEPA, 1994)) that require water utilities to reduce the impact of intermittent discharges on
582 surface waters. Integrated models are often used to demonstrate compliance with regulatory
583 requirements. This work indicates that understanding predictive uncertainty and the role of the

584 risk preferences of individual decision makers could have a significant impact on the cost of
585 such regulatory driven environmental protection programs. It is appreciated there are many
586 more sources of uncertainty in integrated water quality models, such as uncertainty in cost,
587 however not all sources of uncertainty were included as the main aim of the study was to
588 examine the impact of predictive model uncertainty on the risk preferences of individuals
589 involved in the investment decision making process. However, the proposed methodology is
590 flexible and can be adapted to incorporate the impact of other sources of uncertainty on
591 investment decisions to manage systems to ensure regulatory compliance that is determined
592 using performance thresholds.

593

594

595 **6. Acknowledgement**

596 This research work has been supported by the Marie Curie ITN ‘Quantifying Uncertainty in
597 Integrated Catchment Studies (QUICS)’. This project has received funding from the European
598 Union’s Seventh Framework Programme for research, technological development and
599 demonstration under grant agreement no 607000. The authors thank the Luxemburgish
600 *Administration des services techniques de l’agriculture* (ASTA) for the time series of
601 precipitation provided, and to the Observatory for Climate and Environment (OCE) of the LIST
602 for its technical support.

603

604

605 **7. References**

606 Box, G.E.P., Jenkins, G.M., Rinsel, G.C., 2008. Time series analysis: forecasting and control,

607 4th Editio. ed. John Wiley & Sons, Inc.

608 Davis, J.R., Uryasev, S., 2016. Analysis of tropical storm damage using buffered probability
609 of exceedance. *Nat. Hazards* 83, 465–483. <https://doi.org/10.1007/s11069-016-2324-y>

610 De Toffol, S., 2006. Sewer system performance assessment – an indicators based
611 methodology. Leopold Franzens Universität Innsbruck.

612 Delelegn, S.W., Pathirana, A., Gersonius, B., Adeogun, A.G., Vairavamoorthy, K., 2011.
613 Multi-objective optimisation of cost-benefit of urban flood management using a 1D2D
614 coupled model. *Water Sci. Technol.* 63, 1053–1059.
615 <https://doi.org/10.2166/wst.2011.290>

616 Deletic, A., Dotto, C.B.S., McCarthy, D.T., Kleidorfer, M., Freni, G., Mannina, G., Uhl, M.,
617 Henrichs, M., Fletcher, T.D., Rauch, W., Bertrand-Krajewski, J.L., Tait, S., 2012.
618 Assessing uncertainties in urban drainage models. *Phys. Chem. Earth* 42–44, 3–10.
619 <https://doi.org/10.1016/j.pce.2011.04.007>

620 Digman, C., 2018. Personal communication on cost estimates of storage tanks and permeable
621 paving.

622 Dirckx, G., Thoeye, C., De Gueldre, G., Van De Steene, B., 2011. CSO management from an
623 operator’s perspective: A step-wise action plan. *Water Sci. Technol.* 63, 1044–1052.
624 <https://doi.org/10.2166/wst.2011.288>

625 Environment Agency, 2017. Thames Water ordered to pay record £20 million for river
626 pollution [WWW Document]. URL [https://www.gov.uk/government/news/thames-](https://www.gov.uk/government/news/thames-water-ordered-to-pay-record-20-million-for-river-pollution)
627 [water-ordered-to-pay-record-20-million-for-river-pollution](https://www.gov.uk/government/news/thames-water-ordered-to-pay-record-20-million-for-river-pollution) (accessed 11.25.19).

628 Foundation for Water Research, 2012. Urban Pollution Management Manual 3rd Edition
629 [WWW Document]. URL <http://www.fwr.org/UPM3/> (accessed 8.8.16).

630 Heuvelink, G.B.M., Brown, J.D., van Loon, E.E., 2007. A probabilistic framework for
631 representing and simulating uncertain environmental variables. *Int. J. Geogr. Inf. Sci.*
632 21, 497–513. <https://doi.org/10.1080/13658810601063951>

633 Konno, H., Suzuki, K.-I., 1995. A Mean-Variance-Skewness Portfolio Optimization Model.
634 *J. Oper. Res. Soc. Japan* 38, 173–187.

635 Korving, H., Van Noordwijk, J.M., Van Gelder, P., Clemens, F., 2009. Risk-based design of
636 sewer system rehabilitation. *Struct. Infrastruct. Eng.* 5, 215–227.
637 <https://doi.org/10.1080/15732470601114299>

638 Lin, R., Zheng, F., Savic, D., Zhang, Q., Fang, X., 2020. Improving the effectiveness of
639 multi-objective optimization design of urban drainage systems. *Water Resour. Res.*
640 e2019WR026656.

641 Mafusalov, A., Uryasev, S., 2014. Buffered Probability of Exceedance : Mathematical
642 Properties and Optimization Algorithms.

643 Markowitz, H., 1952. Portfolio Selection. *J. Finance* 7, 77–91. [https://doi.org/10.1111/j.1540-](https://doi.org/10.1111/j.1540-6261.1952.tb01525.x)
644 [6261.1952.tb01525.x](https://doi.org/10.1111/j.1540-6261.1952.tb01525.x)

645 McCuen, R.H., 1998. *Hydrologic Analysis and Design*, Second Edi. ed. Prentice Hall.

646 Meng, F., Fu, G., Butler, D., 2016. Water quality permitting: From end-of-pipe to operational
647 strategies. *Water Res.* 101, 114–126. <https://doi.org/10.1016/j.watres.2016.05.078>

648 Milieu, 2016. Assessment of impact of storm water overflows from combined waste water
649 collecting systems on water bodies (including the marine environment) in the 28 EU
650 Member States. European Commission Specific Contract No.
651 070201/2014/SFRA/693725/ENV/C.2.

652 Mohammadiun, S., Yazdi, J., Neyshabouri, S.A.A.S., Sadiq, R., 2018. Development of a

653 stochastic framework to design/rehabilitate urban stormwater drainage systems based on
654 a resilient approach. *Urban Water J.* 15, 167–176.
655 <https://doi.org/10.1080/1573062X.2018.1424218>

656 Moreno-Rodenas, A.M., Tscheikner-Gratl, F., Langeveld, J.G., Clemens, F.H.L.R., 2019.
657 Uncertainty analysis in a large-scale water quality integrated catchment modelling study.
658 *Water Res.* 158, 46–60.

659 Morgan, D., Xiao, L., McNabola, A., 2017. Technologies for monitoring, detecting and
660 treating overflows from urban wastewater networks. EPA Research Report. (2014-W-
661 DS-19). Environmental Protection Agency, Ireland.

662 ÖWAV-Regelblatt 19, 2007. Richtlinien für die Bemessung von Mischwasserentlastungen.
663 Vienna, Austria.

664 Portielje, R., Hvitved-Jacobsen, T., Schaarup-Jensen, K., 2000. Risk analysis using stochastic
665 reliability methods applied to two cases of deterministic water quality models. *Water*
666 *Res.* 34, 153–170. [https://doi.org/10.1016/S0043-1354\(99\)00131-1](https://doi.org/10.1016/S0043-1354(99)00131-1)

667 Reda, A.L.L., Beck, M.B., 1997. Ranking strategies for stormwater management under
668 uncertainty: Sensitivity analysis. *Wat. Sci. Tech.* 36, 357–371.

669 Rico-Ramirez, M.A., Liguori, S., Schellart, A.N.A., 2015. Quantifying radar-rainfall
670 uncertainties in urban drainage flow modelling. *J. Hydrol.* 528, 17–28.

671 Schellart, A.N.A., Tait, S.J., Ashley, R.M., 2010. Towards quantification of uncertainty in
672 predicting water quality failures in integrated catchment model studies. *Water Res.* 44,
673 3893–3904. <https://doi.org/10.1016/j.watres.2010.05.001>

674 Thorndahl, S., Willems, P., 2008. Probabilistic modelling of overflow, surcharge and
675 flooding in urban drainage using the first-order reliability method and parameterization

676 of local rain series. *Water Res.* 42, 455–66. <https://doi.org/10.1016/j.watres.2007.07.038>

677 Torres-Matallana, J.A., Leopold, U., Heuvelink, G.B.M., 2017. Multivariate autoregressive
678 modelling and conditional simulation of precipitation time series for urban water
679 models, in: 10th World Congress on Water Resources and Environment “Panta Rhei.”
680 pp. 299–306.

681 Torres-Matallana, J.A., Leopold, U., Klepiszewski, K., Heuvelink, G.B.M., 2018. EmiStatR:
682 A simplified and scalable urban water quality model for simulation of combined sewer
683 overflows. *Water (Switzerland)* 10. <https://doi.org/10.3390/w10060782>

684 Uryasev, S., 2014. Buffered probability of exceedance and buffered service level: Definitions
685 and properties. *Dep. Ind. Syst. Eng. Univ. Florida, Res. Rep.* 3.

686 USEPA, 1994. NPDES CSO Control Policy [WWW Document]. URL
687 <https://www.epa.gov/npdes/npdes-cso-control-policy>

688 Vrugt, J.A., ter Braak, C.J.F., Diks, C.G.H., Robinson, B.A., Hyman, J.M., Higdon, D., 2009.
689 Accelerating Markov Chain Monte Carlo Simulation by Differential Evolution with
690 Self-Adaptive Randomized Subspace Sampling. *Int. J. Nonlinear Sci. Numer. Simul.* 10,
691 273–290.

692 Welker, A., 2007. Occurrence and fate of organic pollutants in combined sewer systems and
693 possible impacts on receiving waters. *Water Sci. Technol.* 56, 141–148.
694 <https://doi.org/10.2166/wst.2007.755>

695 Yu, J., Qin, X., Asce, A.M., Chiew, Y.M., Asce, M., Min, R., Shen, X., 2017. Stochastic
696 Optimization Model for Supporting Urban Drainage Design under Complexity 143, 1–
697 10. [https://doi.org/10.1061/\(ASCE\)WR.1943-5452.0000806](https://doi.org/10.1061/(ASCE)WR.1943-5452.0000806).

698 Zhang, W., Li, J., Chen, Y., Li, Y., 2019. A Surrogate-Based Optimization Design and

699 Uncertainty Analysis for Urban Flood Mitigation. *Water Resour. Manag.* 33, 4201–
700 4214. <https://doi.org/10.1007/s11269-019-02355-z>.

701